

## Supplementary Materials

Shu Yang<sup>1,2,a</sup>, Keke Zhi<sup>3,4,a</sup>, Zhimin Zhang<sup>1,2</sup>, Rukiya-Kerem<sup>1,2</sup>, Qiong Hong<sup>1,2</sup>, Lei Zhao<sup>1,2</sup>, Wenbo Wu<sup>1</sup>, Lulu

Wang<sup>1,2,\*</sup>, and Duozi Wang<sup>1,2,\*</sup>

1 College of Chemistry, Xinjiang University, Urumqi, 830017, PR China

2 State Key Laboratory of Chemistry and Utilization of Carbon Based Energy Resources, Urumqi, 830017, PR China

3 China University of Petroleum-Beijing at Karamay, Karamay 834000, PR China

4 State Key Laboratory of Heavy Oil Processing-Karamay Branch, Karamay 834000, PR China

\* Correspondence: 316813906@qq.com; Tel.:13579275610; xjwangdz@sina.com

a These authors contribute equally to this work.

### Materials and Reagents:

1,4-dioxane (AR, > 99%) and methanol were sourced from Tianjin Zhiyuan Chemical Reagent Co., Ltd.(Tientsin China), 1-Butanol (AR, > 99%) and 1,2-Dichlorobenzene (AR, > 98%) were sourced from Greagent(Shanghai China), 5-Bromopicolonitrile (AR, > 98%) and 4-Bromobenzonitrile(AR, > 98%) were purchased from Adamas Reagent Co., Ltd. (Shanghai, China), Mesitylene (AR, > 97%) was purchased from Adamas Reagent Co., Ltd. (Shanghai, China), 4-(4,4,5,5-Tetramethyl-1,3,2-dioxaborolan-2-yl)aniline (AR,>98%) was purchased from Adamas Reagent Co., Ltd. (Shanghai, China), Tetrahydrofuran was sourced from Tianjin Zhiyuan Chemical Reagent Co., Ltd.(Tientsin, China), Tetrakis(triphenylphosphine)palladium (AR, > 99%) was purchased from Adamas Reagent Co., Ltd. (Shanghai, China), 4-Formylphenylboronic Acid (AR, > 97%), N,N-dimethylformamide (AR, > 99%) was purchased from Adamas Reagent Co., Ltd. (Shanghai, China), dimethyl-1-pyrroline N-oxide (DMPO) and Cesium Fluoride (AR, > 99%) was purchased from Aladdin Co. Ltd., (Shanghai, China). All chemicals were used without further purification.

### Experimental Section

#### Calculation of average fluorescence lifetime

To shed more light on this issue, the TRPL decay plots were fitted through the biexponential decay function presented as follows:

$$R(t) = B_1 \exp\left(-\frac{t}{\tau_1}\right) + B_2 \exp\left(-\frac{t}{\tau_2}\right)$$

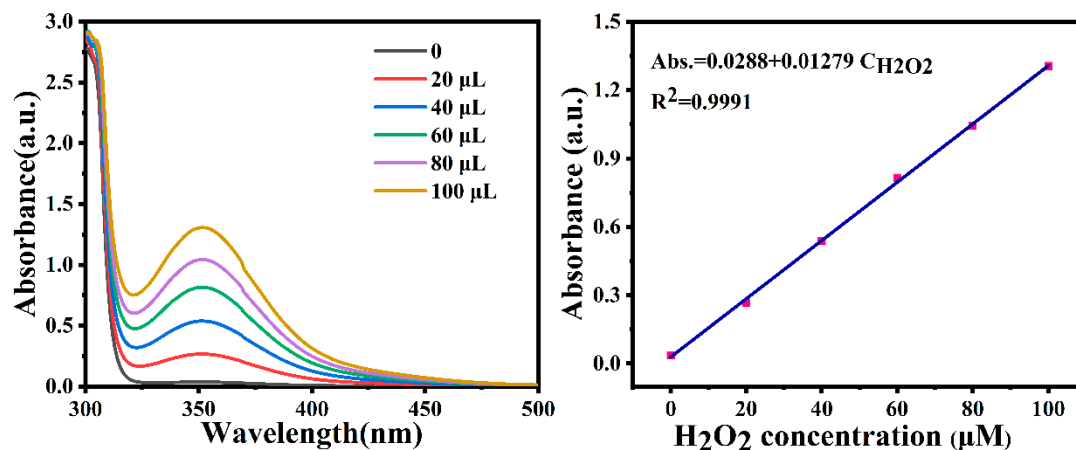
$$\tau_{Ave} = (B_1 \tau_1^2 + B_2 \tau_2^2) / (B_1 \tau_1 + B_2 \tau_2)$$

where B1 and B2 are the weighing factors, and  $\tau_1$  and  $\tau_2$  are the corresponding lifetimes, respectively.

#### H<sub>2</sub>O<sub>2</sub> detection methods.

The amount of H<sub>2</sub>O<sub>2</sub> was determined using iodometry. A solution was prepared by adding 0.5 mL of 0.4 mol L<sup>-1</sup> potassium hydrogen phthalate (C<sub>8</sub>H<sub>5</sub>KO<sub>4</sub>) aqueous solution and 0.5 mL of 0.4 mol L<sup>-1</sup> potassium iodide (KI) aqueous solution. The solution was then kept for 30 min. The H<sub>2</sub>O<sub>2</sub> molecules reacted with iodide anions (I<sup>-</sup>) under acidic

conditions ( $\text{H}_2\text{O}_2 + 3\text{I}^- + 2\text{H}^+ \rightarrow \text{I}_3^- + 2\text{H}_2\text{O}$ ) to produce triiodide anions. The amount of  $\text{H}_2\text{O}_2$  was determined by measuring the absorbance at 352 nm using of UV-vis spectroscopy. The linear calibration curve for  $\text{H}_2\text{O}_2$  concentration was generated by diluting a  $9.12 \text{ mol L}^{-1}$   $\text{H}_2\text{O}_2$  stock solution to cover the range of  $\text{H}_2\text{O}_2$  concentrations (0-100  $\mu\text{M}$ ). The linear relationship between  $\text{H}_2\text{O}_2$  concentration and the absorption intensity was established as follows:



#### Photocatalytic decomposition of $\text{H}_2\text{O}_2$ by COFs.

The photocatalytic consumption of  $\text{H}_2\text{O}_2$  was tested by dispersing COFs-based catalysts (2.5 mg) in an aqueous solution (10 mL) containing  $\text{H}_2\text{O}_2$  (50  $\mu\text{M}$ ) under continuous  $\text{N}_2$  aeration.

#### Cycling Tests.

The tube was filled with 2.5 mg of photocatalyst, 10 mL of  $\text{H}_2\text{O}$ , and sealed with a septum. The resulting suspension was treated with ultrasonication until the photocatalyst was dispersed, and then degassed by bubbling  $\text{O}_2$  for 15 minutes. Next, the mixture solution was stirred under dark conditions for 15 min to achieve the absorption-desorption equilibrium. The reaction mixture was illuminated with 10 W 420 nm LED for 2 h. All the reaction system was kept at  $25^\circ\text{C}$  as controlled by cooling water. After the reaction, the COFs-based photocatalyst was centrifuged, washed with methanol, and dried in a vacuum oven at  $70^\circ\text{C}$  for 12 h. The resulting photocatalyst was then used directly for the subsequent runs.

#### Electrochemical measurements

Electrochemical measurements of the photocatalysts were performed on a standard three-electrode system by an electrochemical workstation (CHI-660D, Shanghai Chenhua, China). The resulting electrode, twisted platinum wire and Ag/AgCl electrode were used as working, counter and reference electrodes, respectively. The 0.5 M  $\text{Na}_2\text{SO}_4$  aqueous solution (pH = 7) was chosen as supporting electrolyte.

Preparation of COF film for electrochemical tests: 5 mg of COF sample was dissolved in a mixed solution of 655  $\mu\text{L}$  ethanol, 325  $\mu\text{L}$   $\text{H}_2\text{O}$  and 20  $\mu\text{L}$  Nafion, and then sonicated for 3 h to form the homogeneous suspension. The obtained suspension was spin-coated on FTO glass, the effective working area of  $1 \text{ cm}^2$ .

### Electron paramagnetic resonance (EPR) measurements

Hydroxyl radical detection: 5,5-dimethyl-1-pyrroline-N-oxide (DMPO) was selected as the trapping agent during the measurements. 50  $\mu\text{L}$  of the  $\text{H}_2\text{O}$  with the 1 mg COF sample was mixed with 5  $\mu\text{L}$  of DMPO trapping agent solution (10 mM). After being irradiated for 300 s with 10 W 420 nm LED visible light, the mixed solution was characterized by an electron spin resonance spectrometer. Superoxide radical detection: 50  $\mu\text{L}$  of the MeOH with the 1 mg COF sample was mixed with 5  $\mu\text{L}$  of DMPO trapping agent solution (10 mM). After being irradiated for 300 s with visible light, then the mixed solution was detected.

### Supplemental Results

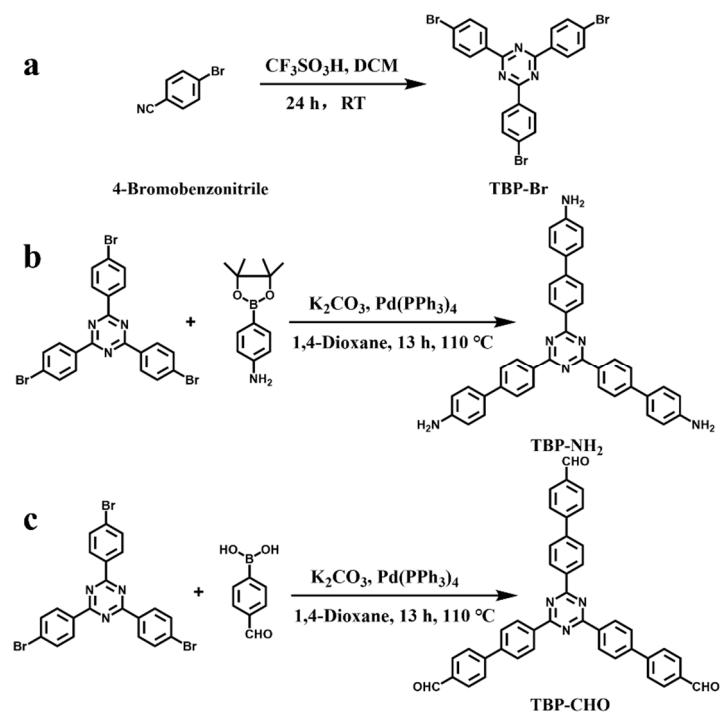


**Figure S1.** Synthesis routes of: (a) TBP-Br; (b) TBP-NH<sub>2</sub>; (c) TBP-CHO.

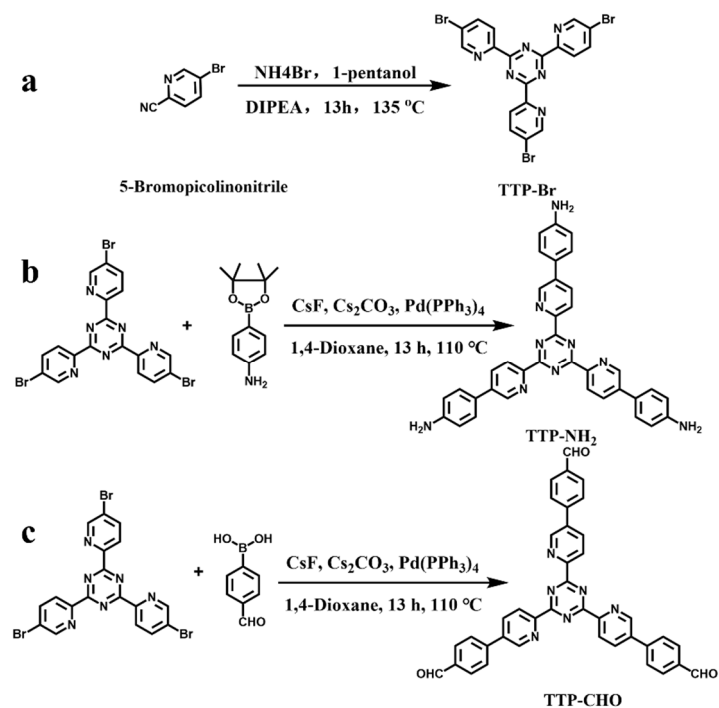


Figure S2. Synthesis routes of: (a) TTP-Br; (b) TTP-NH<sub>2</sub>; (c) TTP-CHO.

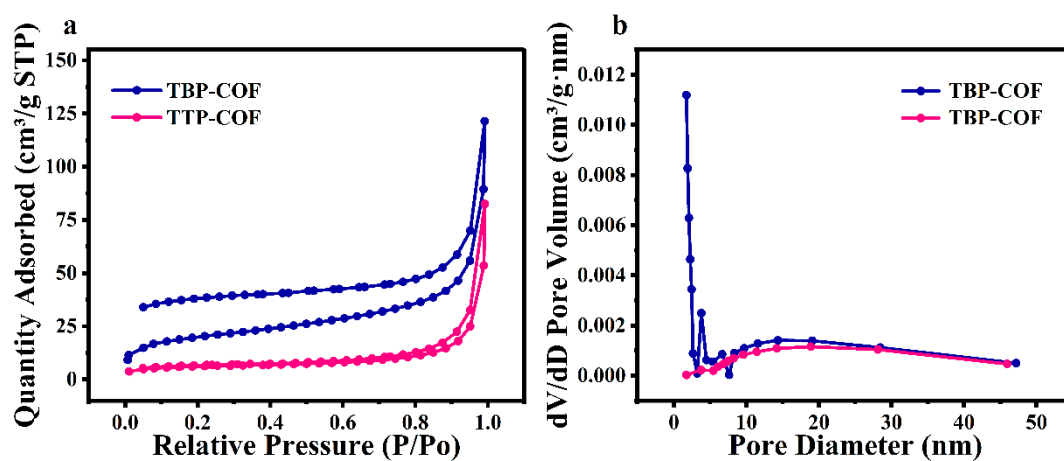


Figure S3. TBP-COF and TTP-COF: (a) N<sub>2</sub> sorption isotherms at 77 K; (b) pore size distributions

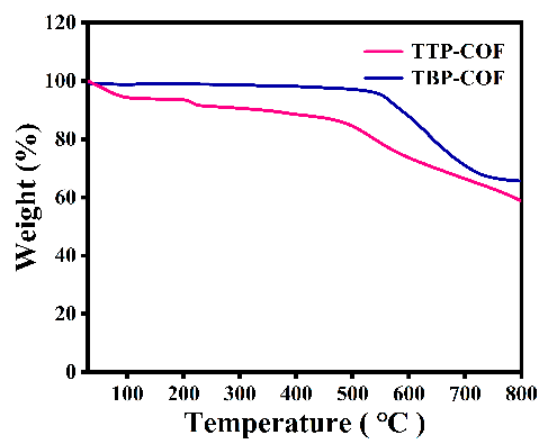


Figure S4. TG curves of TBP-COF and TTP-COF under N<sub>2</sub> atmosphere.

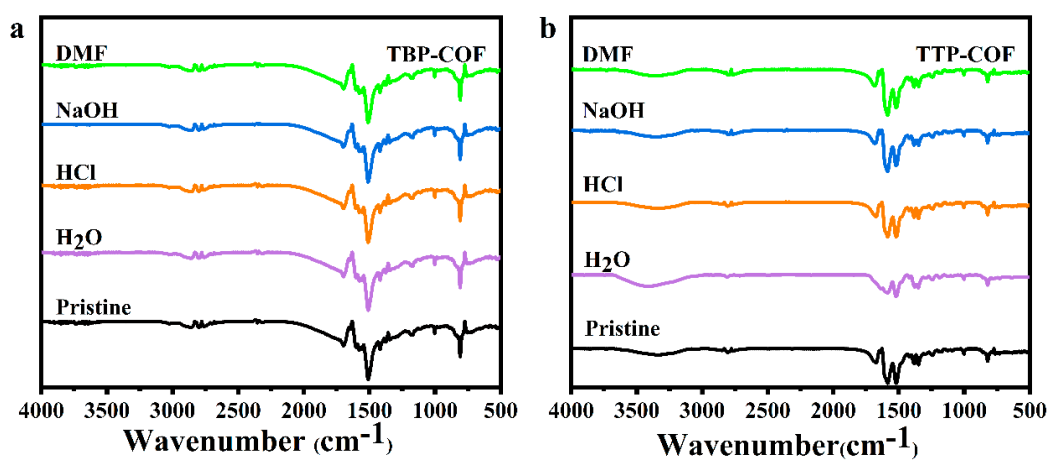
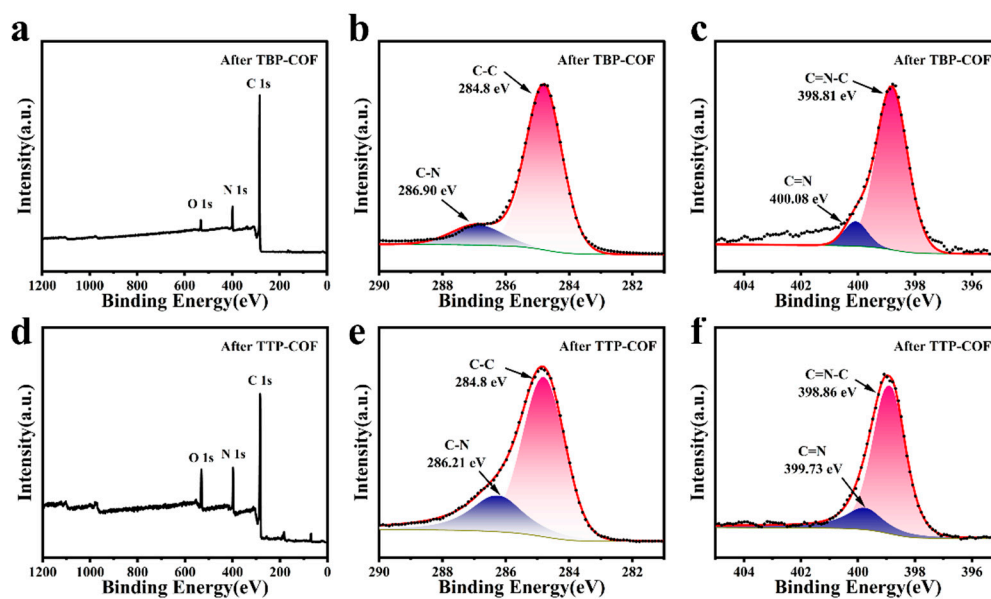
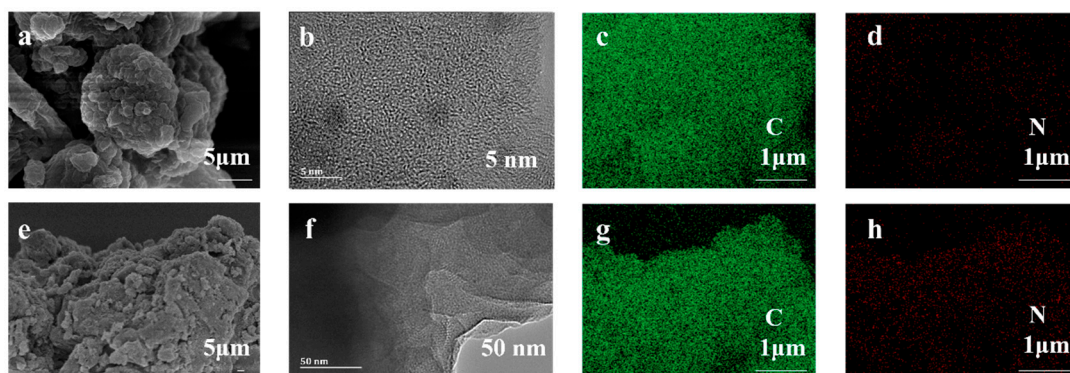


Figure S5. FT-IR patterns of (a) TBP-COF and (b) TTP-COF samples treated at room temperature for 24 h in 1 M of HCl, 1 M of NaOH, H<sub>2</sub>O and DMF. The chemical stability of the COFs was evaluated by soaking the COFs in various solvents such as HCl, NaOH, H<sub>2</sub>O and DMF at concentrations of 0.5 g L<sup>-1</sup>.



**Figure S6.** XPS spectra of TBP-COF after photocatalysis: (a) Survey scan; (b) C 1s; (c) N 1s; XPS spectra of TTP-COF after photocatalysis: (d) Survey scan; (e) C 1s; (f) N 1s.



**Figure S7.** TBP-COF after photocatalysis : (a) SEM; (b) TEM; (c and d) EDS; TTP-COF after photocatalysis : (a) SEM; (b) TEM; (c and d) EDS

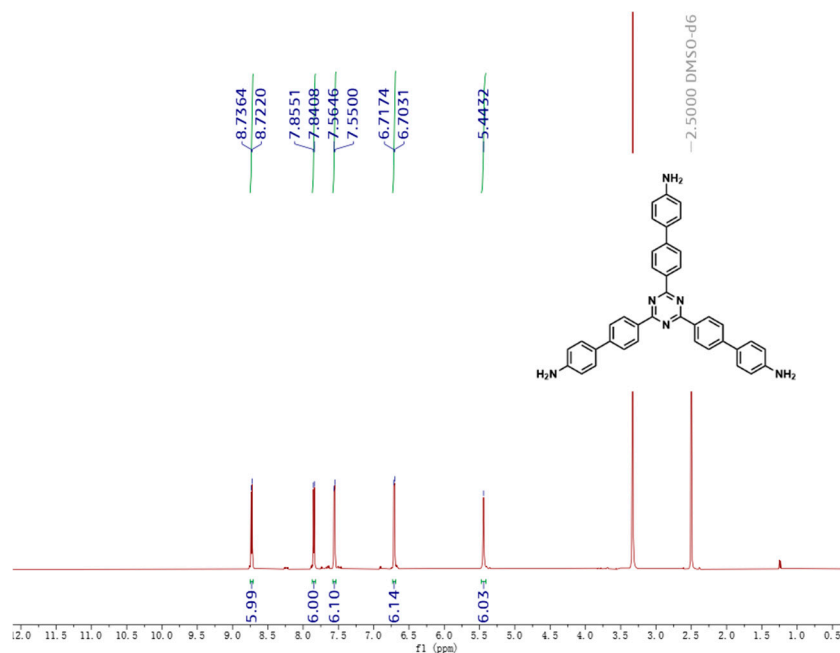


**Figure S8.** <sup>1</sup>H NMR spectra of TBP-NH<sub>2</sub>

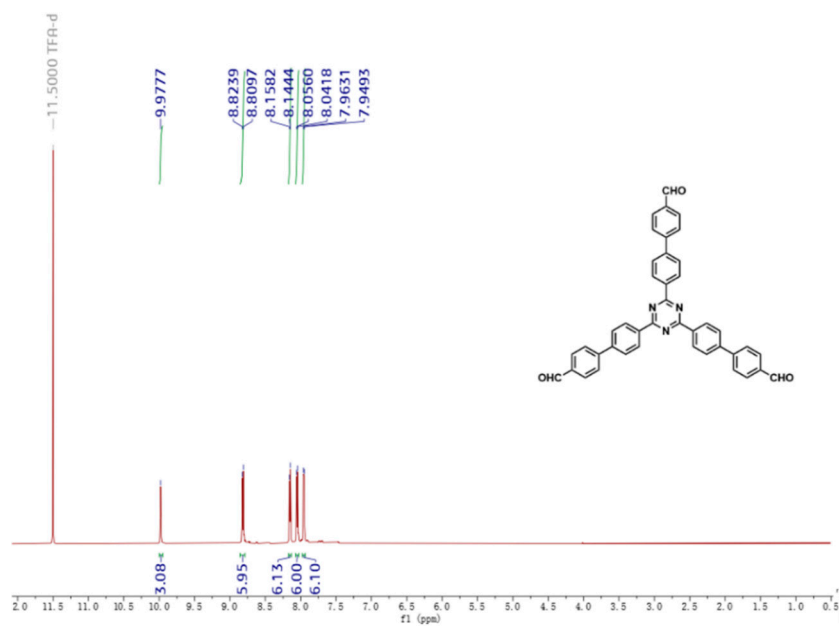


Figure S9. <sup>1</sup>H NMR spectra of TBP-CHO

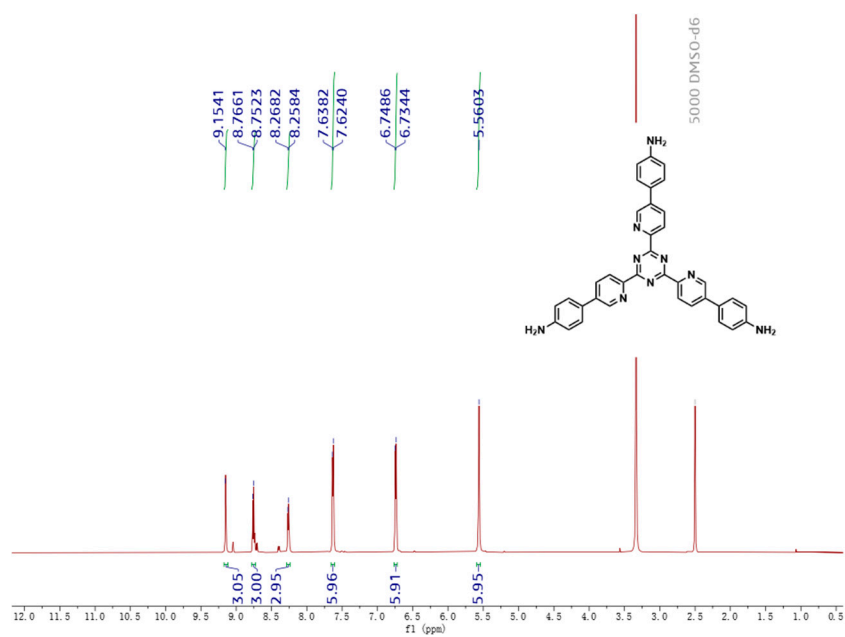


Figure S10. <sup>1</sup>H NMR spectra of TTP-NH<sub>2</sub>

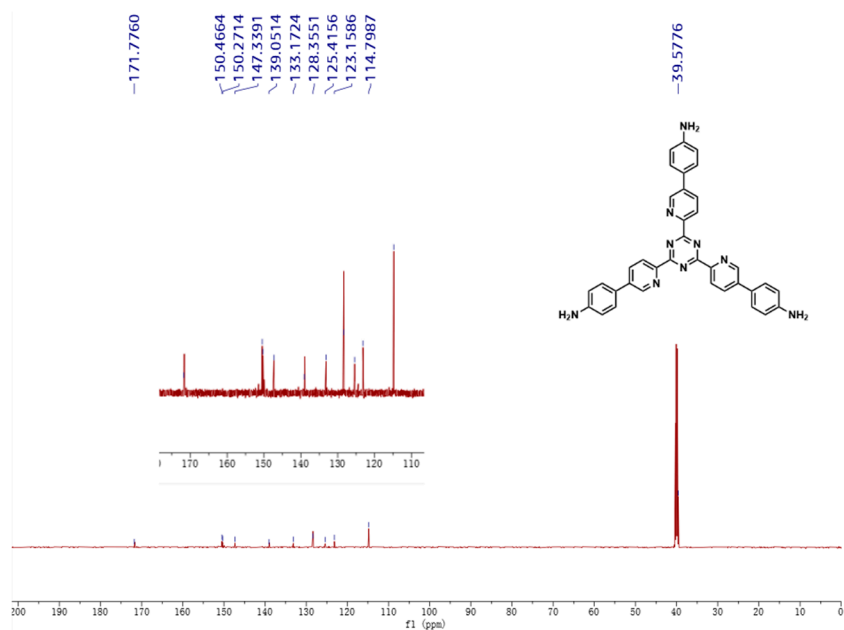


Figure S11. <sup>13</sup>C NMR spectra of TTP-NH<sub>2</sub>

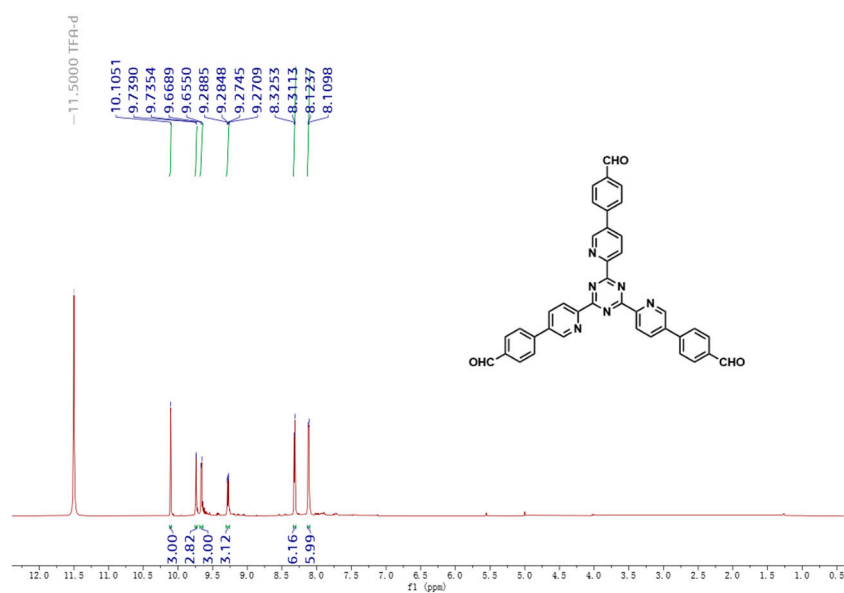
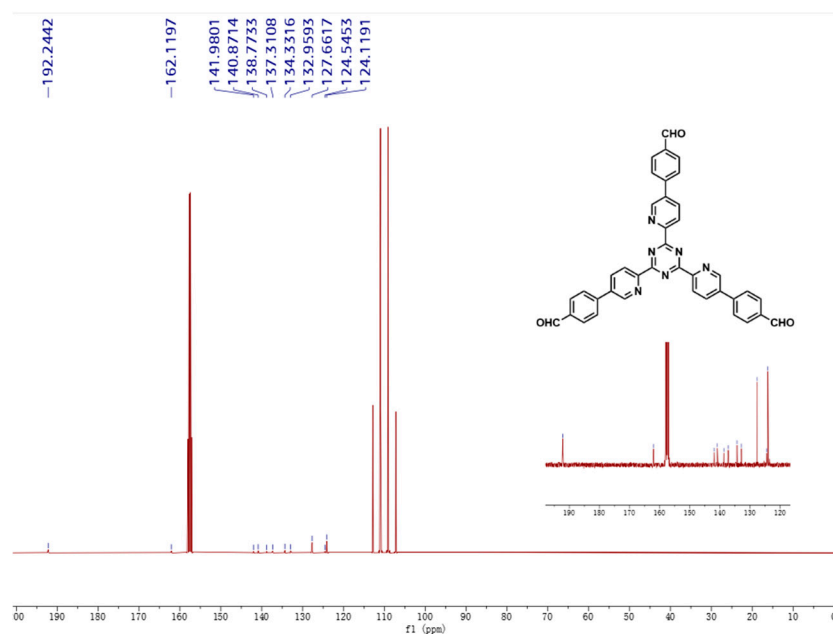


Figure S12. <sup>1</sup>H NMR spectra of TTP-CHO



**Figure S13.**  $^{13}\text{C}$  NMR spectra of TTP-CHO

**Table S1.** Comparison of photocatalytic  $\text{H}_2\text{O}_2$  performance on various representative photocatalysts.

Photocatalyst	Solvent condition	Photocatalytic activity ( $\mu\text{mol g}^{-1} \text{h}^{-1}$ )	Irradiated conditions	Reference
TBP-COF	$\text{H}_2\text{O}$	4244	LED $\lambda=420\text{nm}$	This work
TDB-COF	$\text{H}_2\text{O}$	1868	LED $\lambda=420\text{nm}$	This work
COF-TfpBpy	$\text{H}_2\text{O}$	1042	$\lambda > 420 \text{ nm}$	[1]
SonoCOF-F2	$\text{H}_2\text{O}$	1244	1-sun $\lambda > 420\text{nm}$	[2]
TPB-DMTP-COF	$\text{H}_2\text{O}$	1565	300W Xe $\lambda > 420\text{nm}$	[3]
TF <sub>50</sub> -COF	$\text{H}_2\text{O}$ : EtOH (9:1)	1739	$> 400 \text{ nm}$	[4]
EBA-COF	$\text{H}_2\text{O}$ : EtOH (9:1)	1830	LED $\lambda=420\text{nm}$	[5]
CTF-BPDCN	$\text{H}_2\text{O}$	1944	$\lambda > 420\text{nm}$	[6]
COF TTA-TTTA	$\text{H}_2\text{O}$	2406	50W LED $\lambda=420\text{nm}$	[7]
AQTEE-COP	$\text{H}_2\text{O}$	3204	300W Xe $\lambda > 420\text{nm}$	[8]
FS-COF	$\text{H}_2\text{O}$	3904	300W Xe $\lambda > 420\text{nm}$	[9]
iCOF-DBTP	$\text{H}_2\text{O}$	10010	1-sun $\lambda > 420\text{nm}$	[10]

1. Kou, M.; Wang, Y.; Xu, Y.; Ye, L.; Huo, Y.; Jia, B.; Li, H.; Ren, J.; Deng, Y.; Chen, J. *et al*: Molecularly Engineered Covalent Organic Frameworks for Hydrogen Peroxide Photosynthesis. *Angew Chem Int Ed Engl* **2022**, 61(19):e202200413. [DOI: [10.1002/anie.202200413](https://doi.org/10.1002/anie.202200413)]
2. Zhao, W.; Yan, P.; Li, B.; Bahri, M.; Liu, L.; Zhou, X.; Clowes, R.; Browning, N.D.; Wu, Y.; Ward, J.W. *et al*: Accelerated Synthesis and Discovery of Covalent Organic Framework Photocatalysts for Hydrogen Peroxide Production. *J Am Chem Soc* **2022**, 144(22):9902-9909. [DOI: [10.1021/jacs.2c02666](https://doi.org/10.1021/jacs.2c02666)]
3. Li, L.; Xu, L.; Hu, Z.; Yu, J.C.: Enhanced Mass Transfer of Oxygen through a Gas-Liquid-Solid Interface for Photocatalytic Hydrogen Peroxide Production. *Adv. Funct. Mater* **2021**, 31(52). [DOI: [10.1002/adfm.202106120](https://doi.org/10.1002/adfm.202106120)]
4. Wang, H.; Yang, C.; Chen, F.; Zheng, G.; Han, Q.: A Crystalline Partially Fluorinated Triazine Covalent Organic Framework for Efficient Photosynthesis of Hydrogen Peroxide. *Angew Chem Int Ed Engl* **2022**, 61(19):e20220328. [DOI: [10.1002/anie.20220328](https://doi.org/10.1002/anie.20220328)]
5. Zhai, L.; Xie, Z.; Cui, C.-X.; Yang, X.; Xu, Q.; Ke, X.; Liu, M.; Qu, L.-B.; Chen, X.; Mi, L.: Constructing Synergistic Triazine and Acetylene Cores in Fully Conjugated Covalent Organic Frameworks for Cascade Photocatalytic H<sub>2</sub>O<sub>2</sub> Production. *Chem. Mater.* **2022**, 34(11):5232-5240. [DOI: [10.1021/acs.chemmater.2c00910](https://doi.org/10.1021/acs.chemmater.2c00910)]
6. Chen, L.; Wang, L.; Wan, Y.; Zhang, Y.; Qi, Z.; Wu, X.; Xu, H.: Acetylene and Diacetylene Functionalized Covalent Triazine Frameworks as Metal-Free Photocatalysts for Hydrogen Peroxide Production: A New Two-Electron Water Oxidation Pathway. *Adv Mater* **2020**, 32(2):e1904433. [DOI: [10.1002/adma.201904433](https://doi.org/10.1002/adma.201904433)]
7. Tan, F.; Zheng, Y.; Zhou, Z.; Wang, H.; Dong, X.; Yang, J.; Ou, Z.; Qi, H.; Liu, W.; Zheng, Z. *et al*: Aqueous Synthesis of Covalent Organic Frameworks as Photocatalysts for Hydrogen Peroxide Production. *CCS Chem.* **2022**, 4(12):3751-3761. [DOI: [10.31635/ccschem.022.202101578](https://doi.org/10.31635/ccschem.022.202101578)]
8. Xu, X.; Sa, R.; Huang, W.; Sui, Y.; Chen, W.; Zhou, G.; Li, X.; Li, Y.; Zhong, H.: Conjugated Organic Polymers with Anthraquinone Redox Centers for Efficient Photocatalytic Hydrogen Peroxide Production from Water and Oxygen under Visible Light Irradiation without Any Additives. *ACS Catal.* **2022**, 12(20):12954-12963. [DOI: [10.1021/acscatal.2c04085](https://doi.org/10.1021/acscatal.2c04085)]
9. Luo, Y.; Zhang, B.; Liu, C.; Xia, D.; Ou, X.; Cai, Y.; Zhou, Y.; Jiang, J.; Han, B.: Sulfone-Modified Covalent Organic Frameworks Enabling Efficient Photocatalytic Hydrogen Peroxide Generation Via One-Step Two-Electron O<sub>2</sub> Reduction. *Angew Chem Int Ed Engl* **2023**, 62(26):e202305355. [DOI: [10.1002/anie.202305355](https://doi.org/10.1002/anie.202305355)]
10. Li, G.; Fu, P.; Yue, Q.; Ma, F.; Zhao, X.; Dong, S.; Han, X.; Zhou, Y.; Wang, J.: Boosting Exciton Dissociation by Regulating Dielectric Constant in Covalent Organic Framework for Photocatalysis. *Chem Catalysis* **2022**, 2(7):1734-1747. [DOI: [10.1016/j.checat.2022.05.002](https://doi.org/10.1016/j.checat.2022.05.002)]